Network Topology and the Fragility of Tetrahedral Glass-Forming Liquids

Mark Wilson[1] and Philip S. Salmon[2]

[1]*Department of Chemistry, Physical and Theoretical Chemistry Laboratory, University of Oxford, South Parks Road, Oxford OX1 3QZ, United Kingdom*

[2]*Department of Physics, University of Bath, Bath, BA2 7AY, United Kingdom*

(Received 12 June 2009; published 7 October 2009)

Network-forming liquids comprising tetrahedral motifs are investigated by large-scale molecular dynamics computer simulations within the framework of an ionic interaction model. The network topology is controlled by varying the anion polarizability, which governs the intertetrahedral bond angle, for different system densities. A coupling is found between the growth in magnitude and range of extended range oscillations and the appearance of ordering on an intermediate length scale. The interrelation between the system fragility and the structural arrangements on these two different length scales shows the trends that are observed for glass-forming systems. In particular, the fragility increases with number of edge-sharing motifs.

DOI: 10.1103/PhysRevLett.103.157801 PACS numbers: 61.20.Qg, 61.20.Ja, 61.43.−j, 64.70.P−

The nanoscale ordering in network glass-forming materials at distances larger than the nearest neighbor, and an account of the associated dynamics, are of crucial importance for understanding the process of glass formation along with the general physico-chemical properties of liquids and glasses [1,2]. In general, basic structural units such as tetrahedra link by their corners or edges to give ordering on an intermediate range which manifests itself in the measured diffraction patterns by the appearance of a first sharp diffraction peak (FSDP) at a scattering vector $k_{\mathrm{FSDP}} \simeq 1$–$1.5$ Å^{-1} that is smaller than for the principal peak at $k_{\mathrm{PP}} \simeq 2.1$–$2.7$ Å^{-1} [3,4]. In view of the small k position and sharpness of the FSDP, the associated ordering is often assumed to have the longest range. Recently this viewpoint has, however, been challenged by the observation of extended range ordering in network glasses, of periodicity given by $2\pi/k_{\mathrm{PP}}$, that persists to distances well beyond the domain of the FSDP [5,6]. But what is the relationship, if any, between the structural arrangements on these length scales and the underlying system dynamics? Can the relative ''fragility,'' a measure of the rate at which the dynamical properties of a liquid change on approaching the glass transition [1,7], be rationalized in terms of an interplay between ordering on the intermediate and extended length scales [6,8]?

In this Letter a systematic search is made for a link between the structure and fragility of tetrahedral network forming MX_2 liquids by using large-scale molecular dynamics simulations within the framework of a polarizable ion model (PIM). The anion polarizability, α_X, and system density are used to control the M–X–M bond angle between the structural motifs and hence the network topology while the fragility of the system is assessed by investigating the temperature dependence of the self-diffusion coefficients. We find that when the anion polarization is increased, greater extended range order develops until an alignment occurs in the principal peak positions of the partial structure factors when $\alpha_X = 20$ au. This growth in magnitude and range of the extended range order is accompanied by the appearance of ordering on an intermediate range which shows a coupling between the structural arrangements on these length scales. Moreover, an interrelation is found between the structure and fragility which displays the measured trends. Stronger liquids with a fragility index $m = 20$–28 that are representative of systems such as SiO_2, BeF_2, and GeO_2 [9] occur when the peak position in the M–X–M bond angle distribution from corner-sharing units $\theta^{\mathrm{CS}}_{MXM} = 155$–$120°$ [10,11] which corresponds to $\alpha_X = 0$–10 au. More fragile liquids with $m = 30$–60 that are representative of $ZnCl_2$, $ZnBr_2$ [12], GeS_2 [13], and $GeSe_2$ [14] occur when $\theta^{\mathrm{CS}}_{MXM} = 120$–$85°$ [6,10,15,16] which corresponds to $\alpha_X = 15$–25 au. Once the threshold at $\simeq 120°$ is reached, the fragility increases with number of edge-sharing units, motifs that are often neglected when modeling network properties [17].

The chosen models are based on relatively simple potentials in which the ions interact through pairwise additive Born-Mayer functions [18] augmented by a description of anion polarization using a (dipolar) PIM [19]. The use of computationally tractable energy functions allows access to the appreciable length and time scales required to study ordering on an extended range, which are generally inaccessible to electronic structure methods. In the PIM, α_X controls the M–X–M angle via the presence of induced dipole moments on bridging anions which act to screen the repulsive Coulombic interaction between cations. In extreme cases (large α_X and/or highly polarizing cation) this effect may become large enough to stabilize edge-sharing connections [20]. Anion polarizabilities of between zero (a rigid-ion model or RIM) and 25 au are employed, noting that $\alpha_X = 20$ au corresponds to the model previously used

to best describe $ZnCl_2$ [21]. The simulations were performed using tetragonal cells containing 3270 ions in the NVT ensemble at number densities of 0.01126 and 0.00800 molecules $Å^{-3}$. The higher density allows a direct comparison with the experimentally-determined functions for $ZnCl_2$, while the lower density allows the effect of expanding the network to be investigated. In order to study possible relationships between the underlying network length scales and glass-forming properties, simulations were also performed using 999 ion systems which allowed ion self-diffusion coefficients to be determined from their mean-squared displacements by averaging over time origins for runs of ~2 ns duration.

Figures 1(a)–1(c) show the Faber-Ziman partial structure factors $S_{\alpha\beta}(k)$ (α, $\beta = M$, X), calculated for models using three anion polarizabilities which emphasize differing relationships between the peak positions and hence the inherent length scales. For the RIM ($\alpha_X = 0$) the principal peaks in $S_{MX}(k)$ and $S_{XX}(k)$ are at $k_{PP} \simeq 1.90$ $Å^{-1}$ and $\simeq 1.95$ $Å^{-1}$ whereas $k_{PP} \simeq 1.55$ $Å^{-1}$ for $S_{MM}(k)$. When $\alpha_X = 20$ au, $k_{PP} \simeq 1.98$ $Å^{-1}$ for *all* three functions and an FSDP now appears in $S_{MM}(k)$ at $k_{FSDP} \simeq 1.12$ $Å^{-1}$. The principal peak in $S_{MM}(k)$ for the RIM is therefore "split" to low and high k by the anion polarization to form the PIM function [22]. For $\alpha_X = 25$ au (representative of $GeSe_2$ [15]) the principal peaks in $S_{MX}(k)$, $S_{XX}(k)$ and $S_{MM}(k)$ are at 1.99, 1.97 and 2.14 $Å^{-1}$, respectively. Figure 1(d) shows the evolution of the peak positions in the three partial structure factors as a function of the anion polarizability.

The partial pair distribution functions $g_{\alpha\beta}(r)$ for the $\alpha_X = 20$ and 25 au models display many of the features found experimentally for $ZnCl_2$ [5] and $GeSe_2$ [15], respectively. For example, in the case of $ZnCl_2$ significant ordering on an extended range is observed and each function $rh_{\alpha\beta} \equiv r[g_{\alpha\beta}(r) - 1]$ shares a common wavelength of oscillation given by $a_1 = 2\pi/k_{PP}$. The extended-range oscillations for the different models were fitted at long range to expressions suggested by theory [6,23] of the form $rh_{\alpha\beta}(r) = 2|A_{\alpha\beta}| \exp(-a_0 r)\cos(a_1 r - \theta_{\alpha\beta})$ where a_0^{-1} is a decay length. The results reveal a growth in magnitude and range of the extended range order as α_X is increased from zero to 20 au. A full discussion of these results and the validity of the associated "mixing rules" for the amplitudes, $|A_{\alpha\beta}|$, and phases, $\theta_{\alpha\beta}$, will be undertaken elsewhere [24].

Figure 2 shows the cation self-diffusion coefficient, D, as a function of temperature, T, for selected anion polarizabilities. The data were first fitted to a Vogel-Fulcher-Tammann (VFT) law of the form $D = D_0 \exp[-B/(T - T_0)]$ where B and T_0 control the function curvature and hence characterize the fragility [7,25] (the T_0/B ratio is shown as an inset). The fitted VFT function was then used to generate an effective glass transition temperature, T_f, corresponding to $\ln(D/D_0) = -10$, which was used to scale the temperature axis in Fig. 2 [7]. For both system densities, the fragility increases when $\alpha_X > 15$ au and the high density data show an Arrhenius temperature dependence ($T_0/B = 0$) when $\alpha_X = 15$ au.

Figure 3(a) shows the measured relation between the fragility index m for a variety of MX_2 glass-forming network systems and the peak position θ^{CS}_{MXM} for corner-sharing units in the M–X–M bond angle distribution $n(\theta_{MXM})$. The fragility is small and approximately invariant for high bond angles, characteristic of networks dominated by corner-sharing units in systems like BeF_2, SiO_2, and GeO_2 [6,8,10]. The fragility then increases when

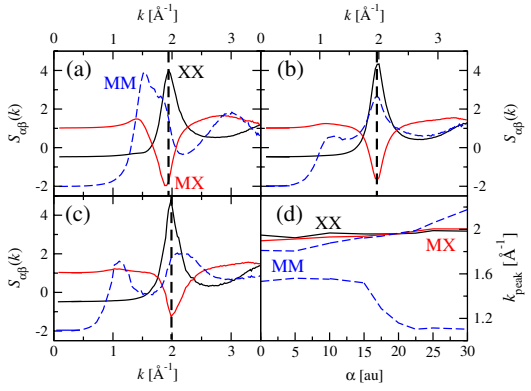

FIG. 1 (color online). The Faber-Ziman partial structure factors, $S_{\alpha\beta}(k)$, for the M–M (broken blue curve), X–X (black curve) and M–X (red curve) correlations as calculated at $T = 900$ K for the high density model with (a) $\alpha_X = 0$ au (RIM), (b) $\alpha_X = 20$ au or (c) $\alpha_X = 25$ au. Vertical dashed lines are drawn to highlight the relative positions of the principal peaks. Panel (d) shows the evolution of the first peak positions in $S_{XX}(k)$ (black curve), $S_{MX}(k)$ (red curve) and $S_{MM}(k)$ (broken blue curves) with α_X. Two curves are plotted for the latter corresponding to the high polarizability FSDP/principal peak and the low polarizability peak-and-shoulder structures.

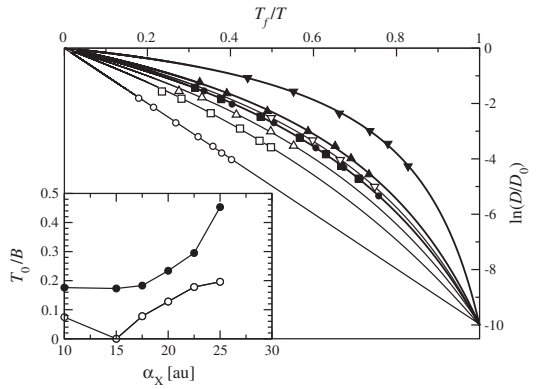

FIG. 2. Dependence of the scaled cation self-diffusion coefficient, D/D_0, on the reduced temperature, T_f/T, for $\alpha_X = 15$ au (○ or ●), 17.5 au (□ or ■), 20 au (△ or ▲) and 25 au (▽ or ▼) where the open and filled symbols correspond to the high and low density simulations, respectively. The lines indicate fits to a VFT expression (see the text). The inset shows the dependence of T_0/B (effectively the system fragility) on α_X for the high (○) and low (●) density models.

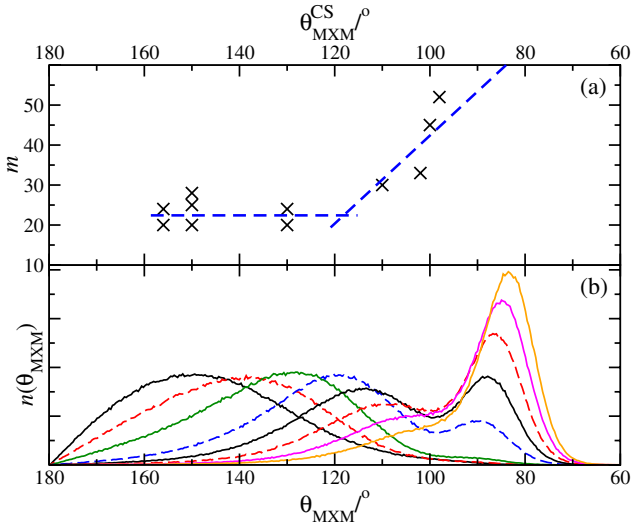

FIG. 3 (color online). (a) Measured fragility index, m, for a series of MX_2 glass-forming systems as a function of θ^{CS}_{MXM}. The measured bond angle data (abscissa, from left to right) correspond to BeF_2 [10], SiO_2 [11], GeO_2 [11], $ZnCl_2$ [10], GeS_2 [16], $ZnBr_2$ (estimated) and $GeSe_2$ [6]. The fragility data are from Refs. [9,12–14]. (b) The M–X–M bond angle distributions calculated from the low density models for $\alpha_X = 0$, 5, 10, 15, 17.5, 20, 22.5 and 25 au (peaks appearing from left to right).

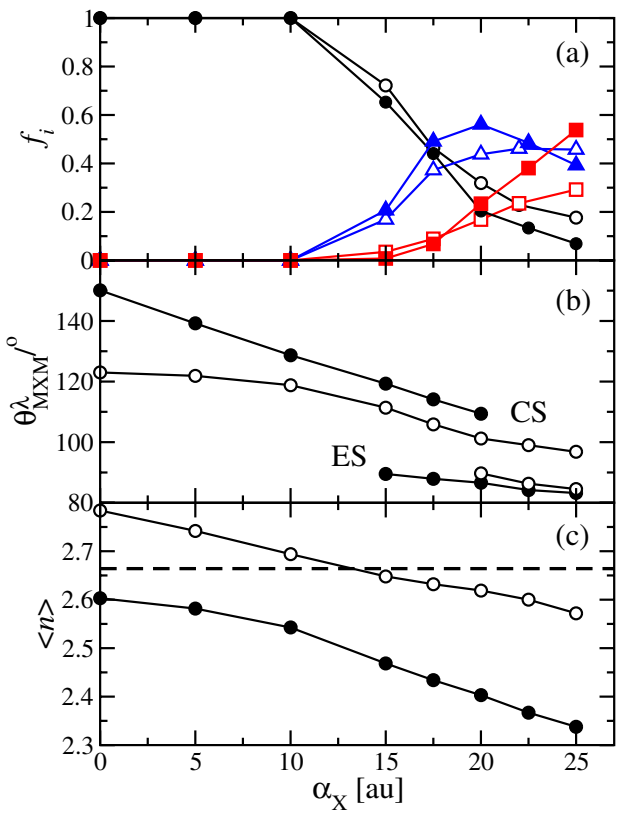

FIG. 4 (color online). Structural properties of the high (open symbols) and low (filled symbols) density models at $T = 900$ K as a function of the anion polarizability α_X. (a) Fraction f_i of corner- and edge-sharing units labeled 0 (○ or ●), 1 (△ or ▲) and 2 (□ or ■). (b) Peak positions θ^{CS}_{MXM} (upper curves) and θ^{ES}_{MXM} (lower curves) in the M–X–M bond angle distribution $n(\theta_{MXM})$ which has two peaks at high α_X values as edge-sharing units become more prolific. (c) The mean coordination number, $\langle n \rangle$, where the horizonal dashed line highlights the ideal tetrahedral network value of $\langle n \rangle = 8/3$ which corresponds to fourfold and twofold coordinated cations and anions, respectively.

$\theta^{CS}_{MXM} \lesssim 120°$ as edge-sharing units become an important feature in systems like GeS_2 and $GeSe_2$ [15,16]. Edge-sharing tetrahedra also appear as dynamic entities in liquid $ZnCl_2$ and $ZnBr_2$ [21,26], the corresponding M–M distances contributing to the low-r side of the first peak in the M–M partial pair distribution function [21] as opposed to forming a distinct peak as in GeS_2 and $GeSe_2$ [15,16]. The simulations also show this trend; e.g., the fragility of the low density model increases when $\alpha_X \gtrsim 15$ au (Fig. 2) as a second peak due to edge-sharing units appears in the M–X–M bond angle distribution at θ^{ES}_{MXM} [Fig. 3(b)].

The evolution with α_X of several structural parameters is shown in Fig. 4 where (a) gives the fraction, f_i, of corner- and edge-sharing units, (b) gives the peak positions θ^{CS}_{MXM} and θ^{ES}_{MXM} in the M–X–M bond angle distribution and (c) gives the mean coordination number $\langle n \rangle$. The structural units in Fig. 4(a) are classified according to their local tetrahedral connectivity [27] where three configurations are possible. Motifs labeled by "0" are purely corner linked, those labeled "1" are linked by a single edge-sharing and two corner-sharing units, while those labeled "2" are linked by two edge-sharing units alone. For both densities studied the fraction of "2" units, f_2, increases strongly for $\alpha_X > 15$ au. Indeed, the most fragile system corresponds to the low density liquid with $\alpha_X = 25$ au which is dominated by such edge-sharing motifs. In this limit the structure has effectively changed from a true three-dimensional network to a pseudo one-dimensional system dominated by polymerlike charge-neutral percolating edge-sharing chains. The change in fragility at high α_X can, therefore, be directly attributed to the formation of edge-sharing units. By comparison, the behavior of the system fragility at low anion polarizabilities appears more complex. For $\alpha_X \lesssim 15$ au the networks are dominated by corner-sharing motifs and it is feasible that the self-diffusion coefficients are related to the mean coordination number. For example, the strongest system corresponds to the high density liquid with $\alpha_X = 15$ au where the network has the least number of defects and $\langle n \rangle \simeq 8/3$ as expected for an ideal tetrahedral network.

In experiment, it is not feasible to vary the M:X ratio for halides like BeF_2 and $ZnCl_2$ or oxides like SiO_2 and GeO_2. However, it is possible to vary the composition in the case of the chalcogenides in order to explore the relation between fragility and edge-sharing motifs. For example, in the case of Ge_xSe_{1-x} ($0 \leq x \leq 1$) viscosity data just above the glass transition temperature T_g show a minimum in the fragility at $x = 0.225$ [28]. This lies within the so-called "intermediate phase" which extends over the range $0.20(1) < x < 0.26(1)$, thus including the composition

$x = 0.2$ where the mean coordination number $\langle n \rangle = 2.4$ [29]. The results from Raman spectroscopy [29,30] and first-principles molecular dynamics simulations [31,32] point to a corresponding reduction in the ratio of edge- to corner-sharing tetrahedra as x is decreased from 0.33 to 0.2. In the case of the Ge-S system, diffraction experiments on the glass also show a reduction in the fraction of edge-sharing units from 0.44(3)–0.47(5) at $x = 0.33$ to 0.32(3) at $x = 0.2$ while Raman scattering experiments show the appearance of S_8 rings for $x \lesssim 0.2$ [16,33]. Viscosity data show a decrease in fragility of the Ge_xS_{1-x} system as x is reduced from 0.33 to 0.30 [13] whereas low frequency Raman spectroscopy measurements on the glass indicate an increase in fragility as x is reduced from 0.33 to 0.2 [34]. Further experiments are therefore required in order to better establish the fragility of the Ge-S system and the role played by S_8 rings. Indeed, it would also be useful to characterize the fragility of both the Ge-Se and Ge-S systems with increasing pressure since a transformation from edge- to corner-sharing tetrahedra is indicated by experiment [16,35]. In the case of the ternary glass-forming system Ge-As-Se, a fragility minimum is reported for several compositions with $\langle n \rangle = 2.4$ [36]. In this material, and in fluorozirconate liquids near T_g, edge-sharing polyhedra are regarded as fragile structural elements [36,37].

In summary, the relation between the structure and fragility of tetrahedral glass-forming liquids has been explored by using large-scale molecular dynamics simulations with a polarizable ion model. The results show ordering on intermediate and extended length scales that is fully consistent with experimental diffraction data. The system fragility systematically increases when the anion polarizability $\alpha_X > 15$ au, matching the trends that are observed experimentally. This increase in fragility is correlated with an increase in number of edge-sharing units, thus emphasizing the importance of these configurations in tetrahedral glass-forming liquids. It would be informative to extend the present molecular dynamics approach to explore the relation between network topology and dynamics in modified network glass-forming systems such as Na_2O–SiO_2 where the fragility increases when a modifier is added [38]. The methodology can also be used to investigate more fragile ionic glass-forming systems such as KCl–$BiCl_3$ [39] and $Ca_2K_3(NO_3)_7$ [40] where $m \simeq 85$–93 [38].

[1] C. A. Angell, J. Non-Cryst. Solids **73**, 1 (1985).
[2] G. N. Greaves and S. Sen, Adv. Phys. **56**, 1 (2007).
[3] S. R. Elliott, Nature (London) **354**, 445 (1991).
[4] P. S. Salmon, Proc. R. Soc. A **445**, 351 (1994).
[5] P. S. Salmon *et al.*, Nature (London) **435**, 75 (2005).
[6] P. S. Salmon, J. Phys. Condens. Matter **17**, S3537 (2005); **18**, 11 443 (2006); **19**, 455208 (2007).
[7] S. Sastry, Nature (London) **409**, 164 (2001).
[8] P. S. Salmon *et al.*, Phys. Rev. Lett. **96**, 235502 (2006); J. Phys. Condens. Matter **19**, 415110 (2007).
[9] V. N. Novikov, Y. Ding, and A. P. Sokolov, Phys. Rev. E **71**, 061501 (2005).
[10] J. A. E. Desa *et al.*, J. Non-Cryst. Solids **51**, 57 (1982).
[11] J. Neuefeind and K.-D. Liss, Ber. Bunsen-Ges. Phys. Chem. **100**, 1341 (1996).
[12] E. A. Pavlatou *et al.*, J. Phys. Chem. B **101**, 8748 (1997).
[13] J. Málek and J. Shánělová, J. Non-Cryst. Solids **243**, 116 (1999).
[14] J. Ruska and H. Thurn, J. Non-Cryst. Solids **22**, 277 (1976).
[15] I. Petri, P. S. Salmon, and H. E. Fischer, Phys. Rev. Lett. **84**, 2413 (2000); P. S. Salmon and I. Petri, J. Phys. Condens. Matter **15**, S1509 (2003).
[16] A. Zeidler *et al.*, J. Phys. Condens. Matter (to be published).
[17] A. Sartbaeva, S. A. Wells, A. Huerta, and M. F. Thorpe, Phys. Rev. B **75**, 224204 (2007).
[18] M. J. L. Sangster and M. Dixon, Adv. Phys. **25**, 247 (1976).
[19] P. A. Madden and M. Wilson, Chem. Soc. Rev. **25**, 339 (1996).
[20] M. Wilson and P. A. Madden, Mol. Phys. **92**, 197 (1997); M. Wilson and M. C. C. Ribeiro, Mol. Phys. **96**, 867 (1999).
[21] B. K. Sharma and M. Wilson, Phys. Rev. B **73**, 060201 (2006).
[22] M. Wilson and P. A. Madden, Phys. Rev. Lett. **72**, 3033 (1994); **80**, 532 (1998).
[23] R. J. F. Leote de Carvalho and R. Evans, Mol. Phys. **83**, 619 (1994).
[24] M. Wilson and P. S. Salmon (to be published).
[25] K. Binder and W. Kob, *Glassy Materials and Disordered Solids* (World Scientific, Singapore, 2005).
[26] S. N. Yannopoulos *et al.*, J. Chem. Phys. **118**, 3197 (2003).
[27] C. Massobrio and A. Pasquarello, Phys. Rev. B **75**, 014206 (2007).
[28] S. Stølen, T. Grande, and H.-B. Johnsen, Phys. Chem. Chem. Phys. **4**, 3396 (2002).
[29] P. Boolchand, X. Feng, and W. J. Bresser, J. Non-Cryst. Solids **293–295**, 348 (2001).
[30] M. Jin *et al.*, Phys. Rev. B **78**, 214201 (2008).
[31] C. Massobrio and A. Pasquarello, Phys. Rev. B **77**, 144207 (2008).
[32] C. Massobrio *et al.*, Phys. Rev. B **79**, 174201 (2009).
[33] E. Bychkov *et al.*, J. Non-Cryst. Solids **352**, 63 (2006).
[34] Y. Wang, M. Nakamura, O. Matsuda, and K. Murase, J. Non-Cryst. Solids **266–269**, 872 (2000).
[35] F. Wang *et al.*, Phys. Rev. B **71**, 174201 (2005); Q. Mei *et al.*, Phys. Rev. B **74**, 014203 (2006).
[36] M. Tatsumisago *et al.*, Phys. Rev. Lett. **64**, 1549 (1990).
[37] C. A. Angell and C. C. Phifer, Mater. Sci. Forum **32–33**, 373 (1988).
[38] Q. Qin and G. B. McKenna, J. Non-Cryst. Solids **352**, 2977 (2006).
[39] J. C. Wasse and P. S. Salmon, J. Phys. Condens. Matter **10**, 8139 (1998).
[40] M. C. C. Ribeiro, Phys. Rev. B **61**, 3297 (2000).